Transcriptome analysis of Pv11 cells infers the mechanism of desiccation tolerance and recovery

Takahiro G Yamada[1], Yoshitaka Suetsugu[2,†], Ruslan Deviatiiarov[3], Oleg Gusev[3,4], Richard Cornette[2], Alexander Nesmelov[3], Noriko Hiroi[5], Takahiro Kikawada[2,6,*], and Akira Funahashi[1,*]

[1]Department of Biosciences and Informatics, Keio University, Yokohama, Kanagawa, Japan, 223-8522
[2]Institute of Agrobiological Sciences, NARO, Tsukuba, Ibaragi, Japan, 305-8634
[3]Kazan Federal University, Kazan, Respublika Tatarstan, Russia, 420008
[4]RIKEN, Wako, Saitama, Japan, 351-0198
[5]Faculty of Pharmacy, Sanyo-onoda City University, Onoda, Yamaguchi, Japan, 756-0884
[6]Graduate School of Frontier Sciences, The University of Tokyo, Kashiwa, Chiba, Japan, 277-8562
[*]kikawada@affrc.go.jp and funa@bio.keio.ac.jp
[†]Deceased

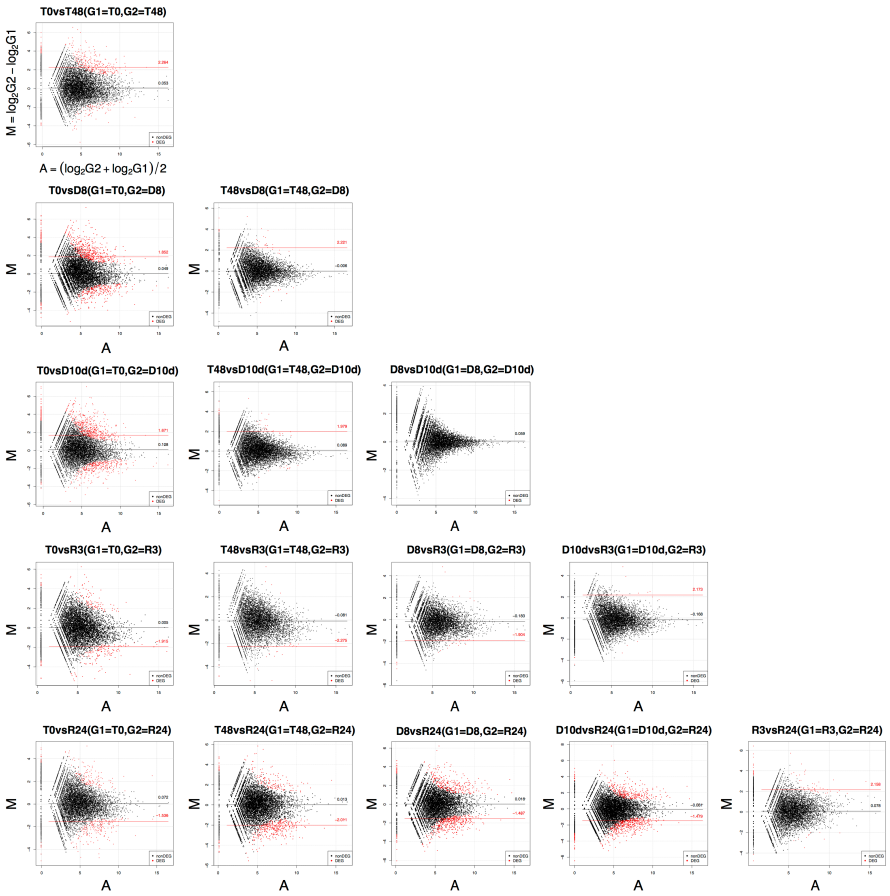

Supplementary Figure S1. M-A plots of DEGs for each pair of samples. The M value indicates the log ratio (sample group 2 (G2) relative to sample group 1 (G1)). The A value indicates the average expression of a gene in samples G1 and G2. The median M values are indicated by black lines for non-DEGs and red lines for DEGs.

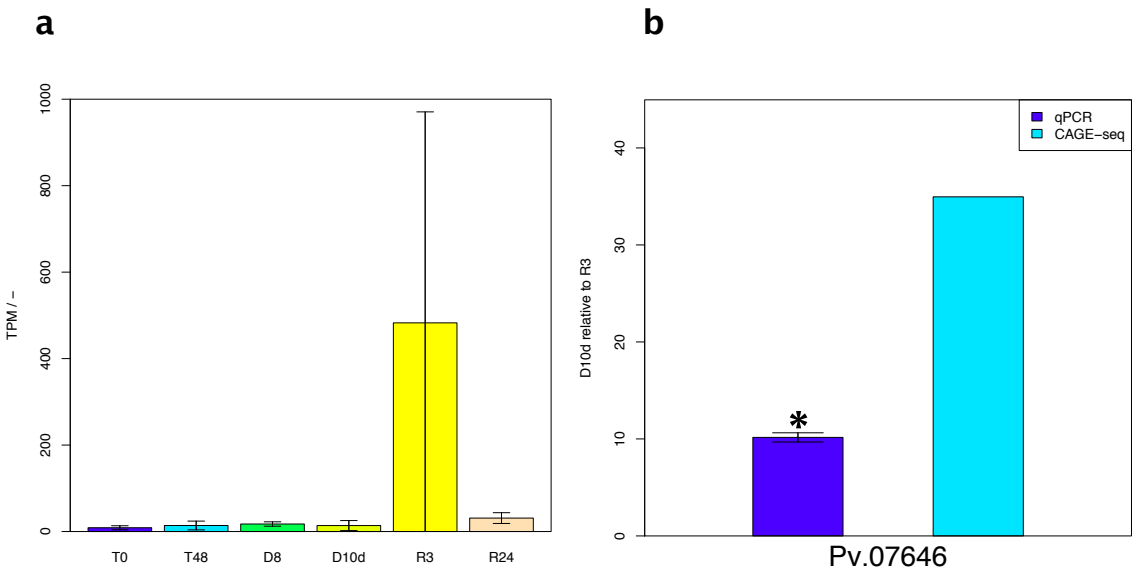

Supplementary Figure S2. The expression of Pv.07646 in each sample quantified by RNA-seq and RT qPCR. a) The expression of Pv.07646, annotated by GO:0036055 (protein-succinyllysine desuccinylase activity) and GO:0036049 (peptidyl-lysine desuccinylation). Horizontal axis shows sample names. TPM, tags per million. Data are mean $\pm$ SD. b) Fold change from R3 to D10d as determined by RT qPCR and CAGE-seq. Asterisk means significant change by Welch's t test (p-value < 0.05).

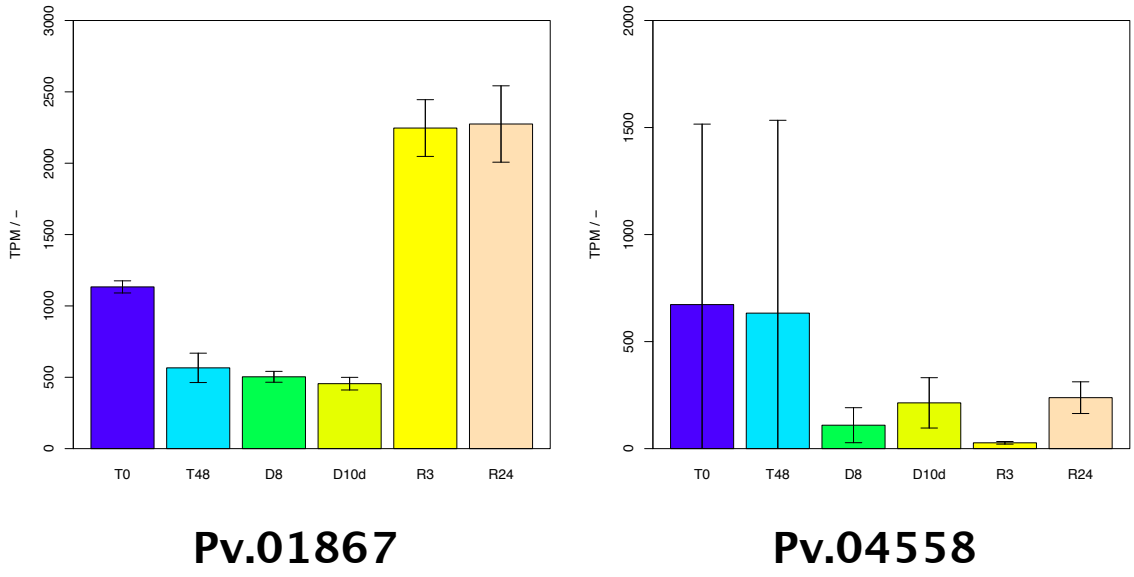

Supplementary Figure S3. Expression of Pv.01867 and Pv.04558. Data are mean ± SD.

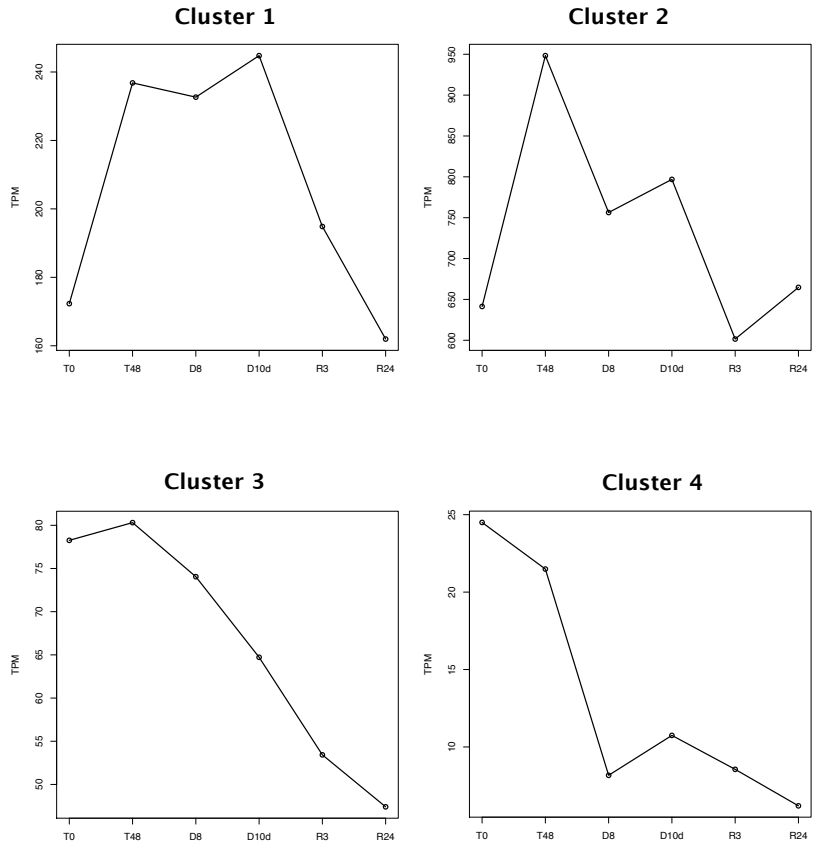

Supplementary Figure S4. Time course of the expression of DEGs annotated by GO:0008152 (metabolic process).

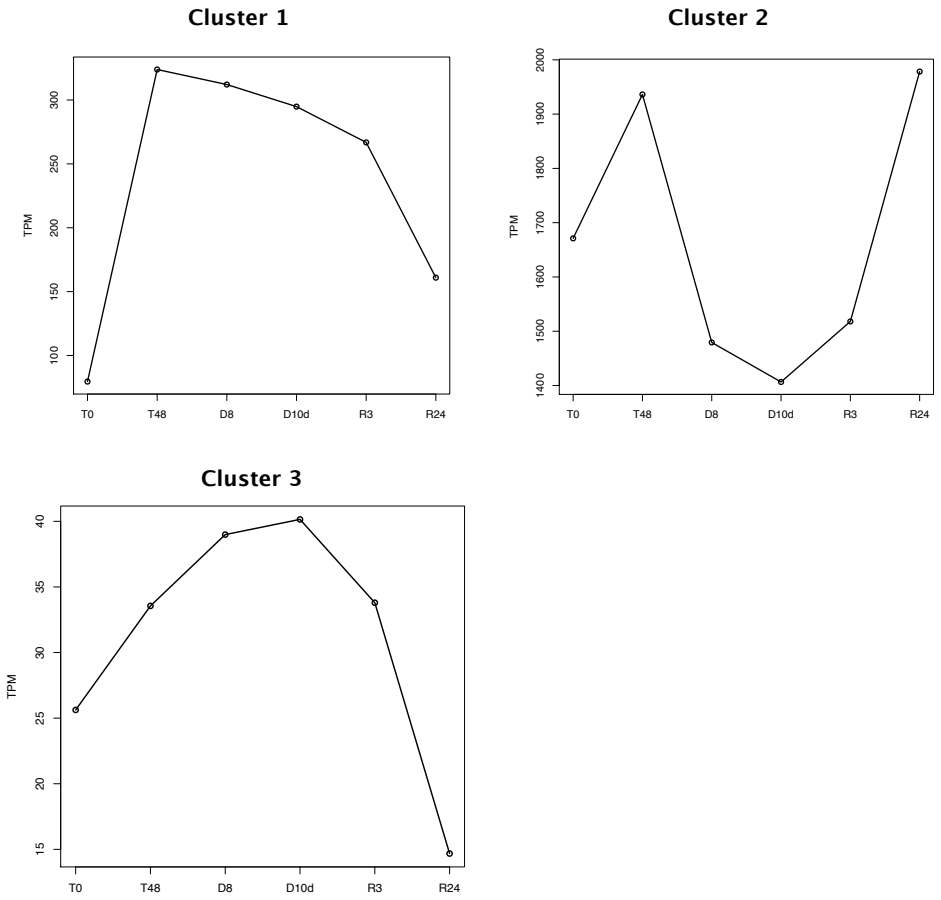

Supplementary Figure S5. Time course of the expression of DEGs annotated by GO:0055114 (oxidation-reduction process).

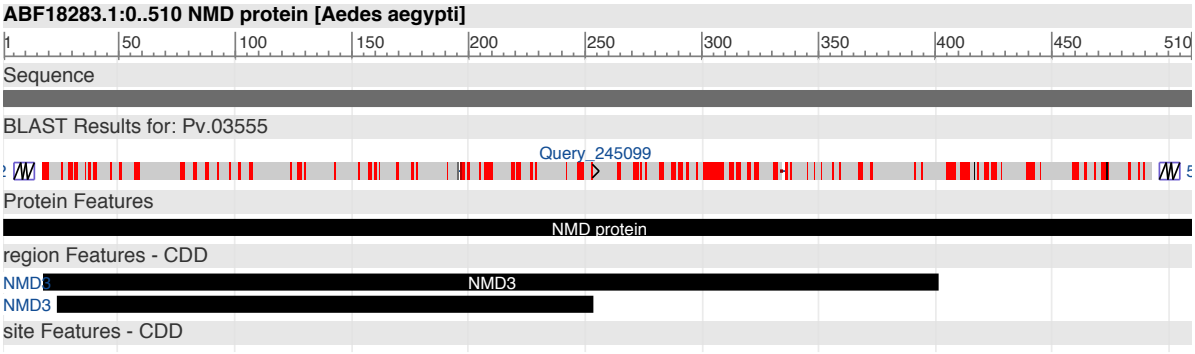

Supplementary Figure S6. Alignment of Pv.03555 with the NMD protein.The visualization by MSAViewer included the sequence of a subject gene as "sequence", the alignment results between the *P. vanderplanki* gene and the subject gene as "BLAST results", specific regions of the subject gene as "region Features - CDD (Conserved Domain Database)", and specific sites of the subject gene as "site Features - CDD". Under "BLAST results", gaps were represented as thick dark red horizontal lines, insertions as black vertical bars and black arrowheads, and aligned regions as grey bars (match regions) or red bars (mismatch regions). The regions and sites of the subject gene that overlapped with those of the aligned *P. vanderplanki* gene were considered present.

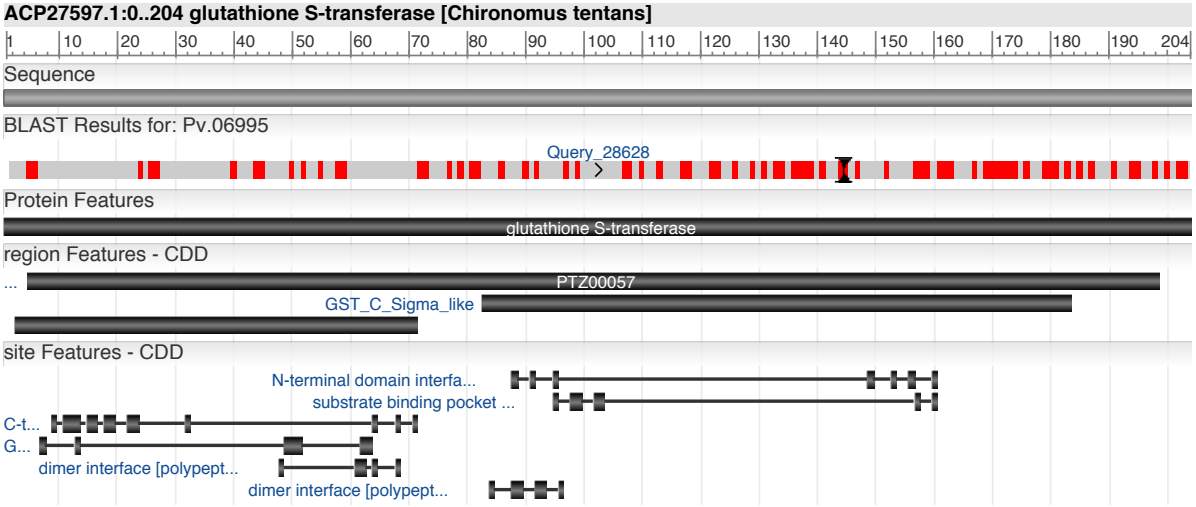

Supplementary Figure S7. Alignment of Pv.06995 with glutathione S-transferase.

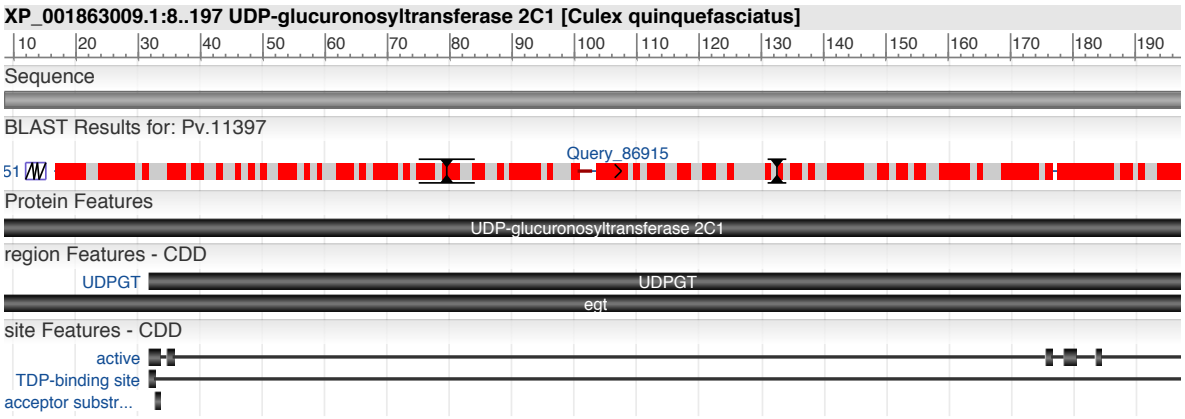

Supplementary Figure S8. Alignment of Pv.11397 with UDP-glucuronosyltransferase 2C1.

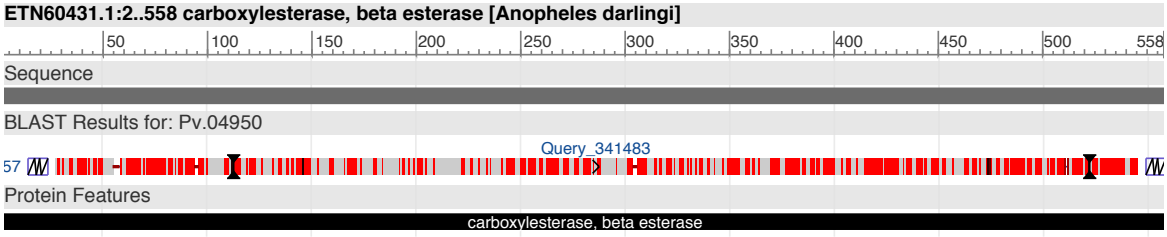

Supplementary Figure S9. Alignment of Pv.04950 with carboxylesterase, beta esterase.

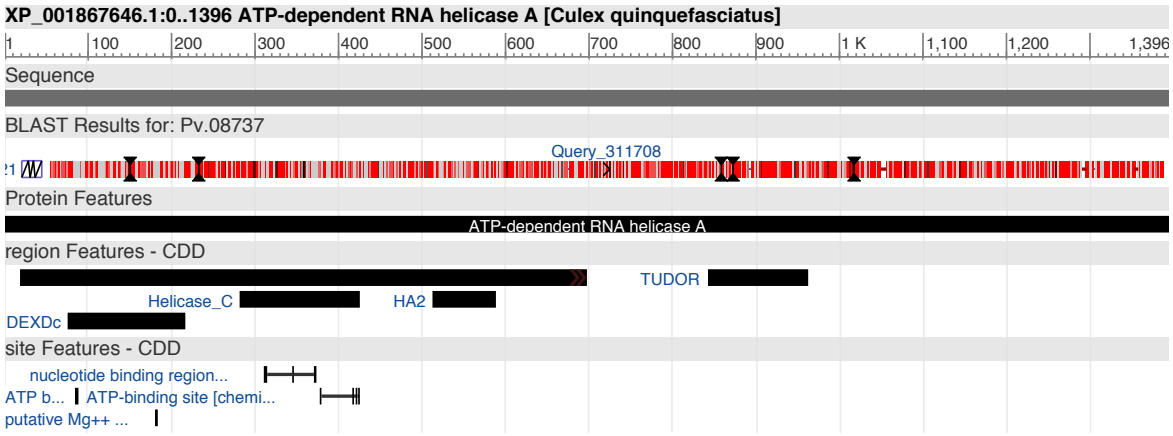

Supplementary Figure S10. Alignment of Pv.08737 with ATP-dependent RNA helicase A.

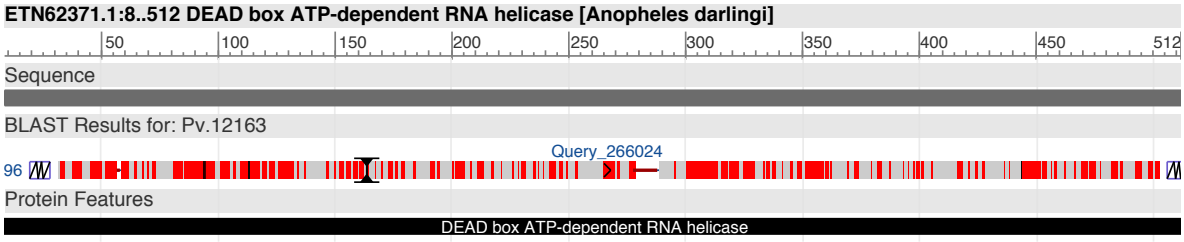

Supplementary Figure S11. Alignment of Pv.12163 with DEAD-box ATP-dependent RNA helicase.

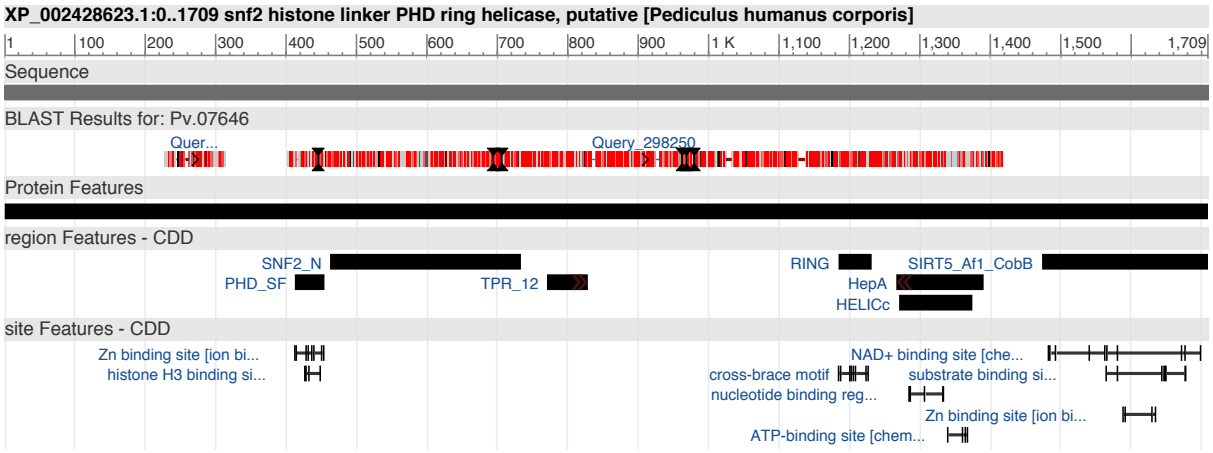

Supplementary Figure S12. Alignment of Pv.07646 with SNF2 histone linker PHD-ring helicase, annotated as putatively involved in desuccinylation.

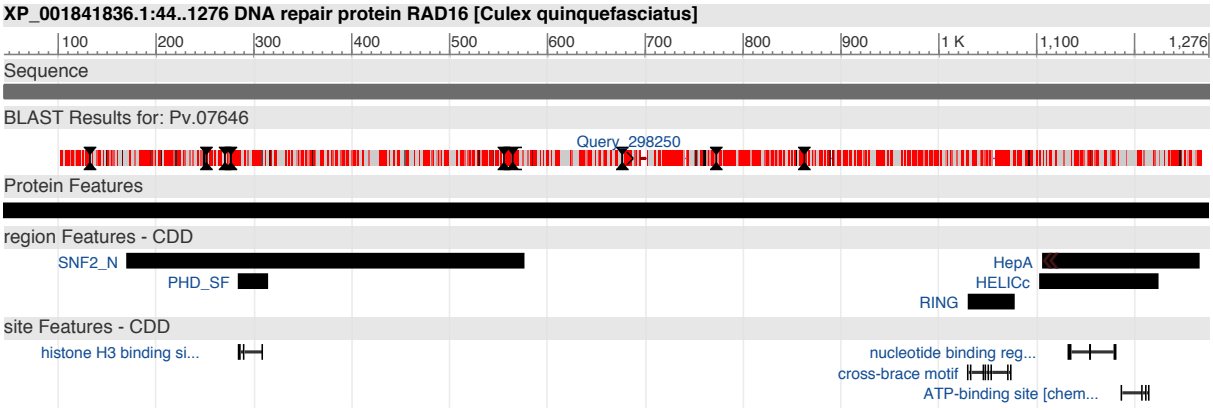

Supplementary Figure S13. Alignment Pv.07646 with the DNA-repair protein RAD16.

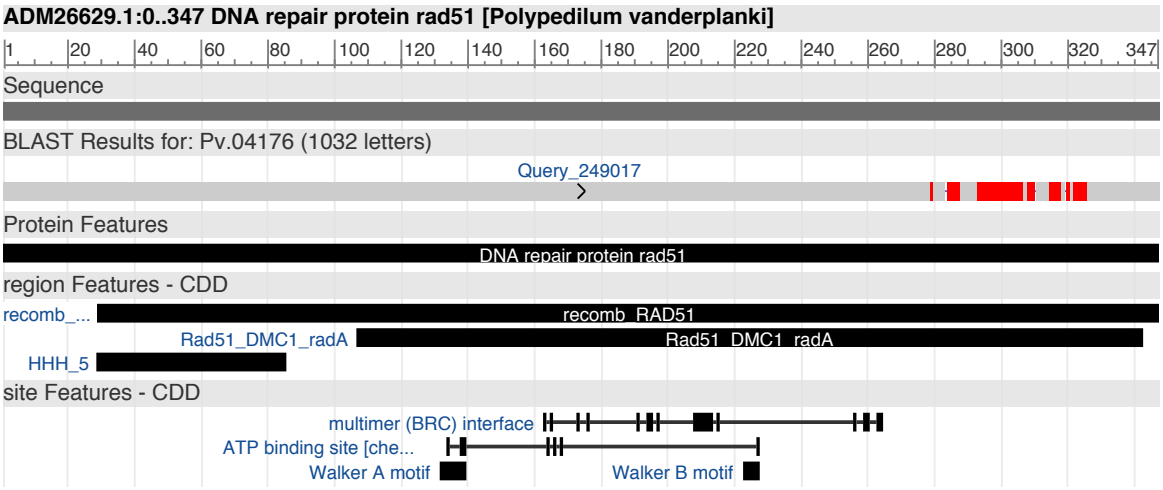

Supplementary Figure S14. Alignment of Pv.04176 with the DNA repair protein Rad51.

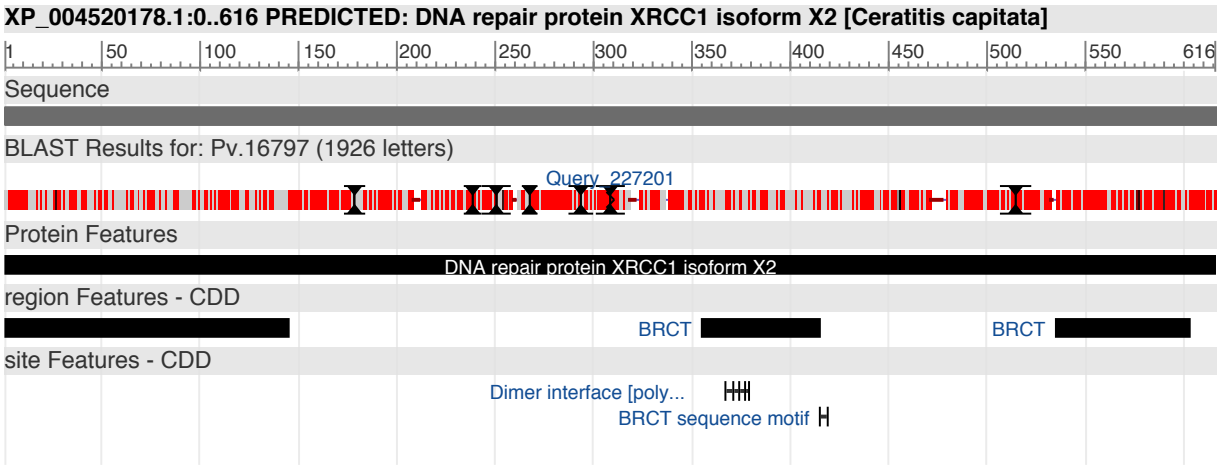

Supplementary Figure S15. Alignment of Pv.16797 with the DNA repair protein XRCC1 isoform X2.

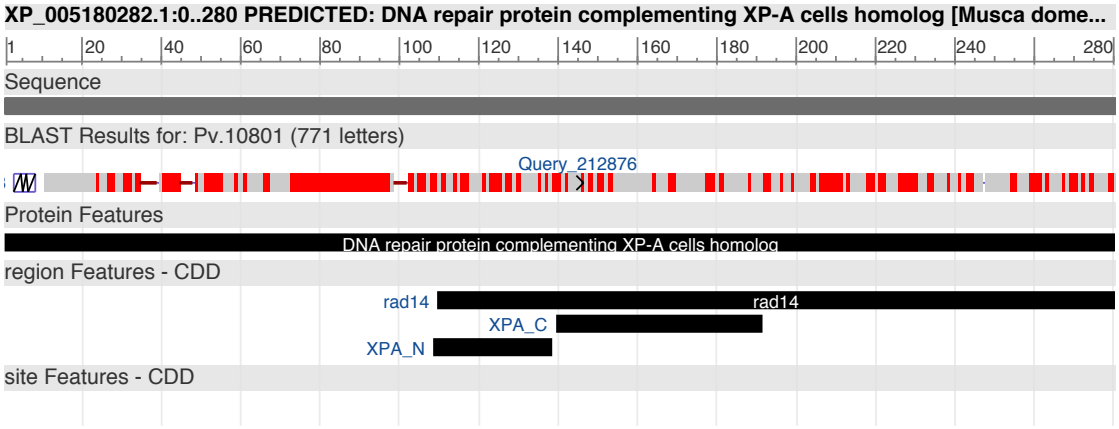

Supplementary Figure S16. Alignment of Pv.10801 with the DNA repair protein complementing XP-A cells homolog.

Supplementary Table S1. DEGs between D10d and R3.

	PvGene ID	Gene Identifier	BLAST first hit gene	E.value
Upregulated in R3	Pv.04891	194753680	GF12734	1.71E-9
	Pv.07646	170027903	DNA repair protein RAD16	0.0
	Pv.01911	765338102	AAEL005023-PA	1.17E-56
	Pv.00327	170050025	conserved hypothetical protein	2.20E-61
	Pv.08602	668455465	AGAP001139-PA-like protein	3.67E-102
	Pv.01867	157136676	AAEL013609-PA, partial	0.0
	Pv.03099		No Hits	
Downregulated in R3	Pv.04558	170036404	conserved hypothetical protein	2.62E-107
	Pv.08152		No Hits	
	Pv.11244	157128927	AAEL011272-PA, partial	2.15E-126
	Pv.13360	170052229	FAM96B	7.93E-77
	Pv.05172	157104834	AAEL004151-PB	4.96E-25
	Pv.13909	751792306	PREDICTED: Y+L amino acid transporter 2	0.0
	Pv.10501	170050626	cyclin b	1.49E-109

Supplementary Table S2. Enriched GOs in DEGs between D10d and R3 (Fisher's exact test, Benjamini–Hochberg method, FDR<0.05). GO, gene ontology ID; Ont, type of ontology (BP, biological process; MF, molecular function; CC, cellular component).

Experiment Condition	GO	GO Description	Ont	FDR
D10dvsR3	GO:0048763	calcium-induced calcium release activity	MF	0.0151449737833333
	GO:0032237	activation of store-operated calcium channel activity	BP	0.0151449737833333
	GO:0030478	actin cap	CC	0.0151449737833333
	GO:0070252	actin-mediated cell contraction	BP	0.0151449737833333
	GO:0036054	protein-malonyllysine demalonylase activity	MF	0.0151449737833333
	GO:0036055	protein-succinyllysine desuccinylase activity	MF	0.0151449737833333
	GO:0036047	peptidyl-lysine demalonylation	BP	0.0151449737833333
	GO:0036049	peptidyl-lysine desuccinylation	BP	0.0151449737833333
	GO:0005826	actomyosin contractile ring	CC	0.0302127188827813
	GO:0030589	pseudocleavage involved in syncytial blastoderm formation	BP	0.0367338112067659
	GO:0090254	cell elongation involved in imaginal disc-derived wing morphogenesis	BP	0.0367338112067659
	GO:0045495	pole plasm	CC	0.0367338112067659
	GO:0045178	basal part of cell	CC	0.0385983590140961
	GO:0017146	N-methyl-D-aspartate selective glutamate receptor complex	CC	0.0385983590140961
	GO:0051533	positive regulation of NFAT protein import into nucleus	BP	0.0401298171424475
	GO:0018345	protein palmitoylation	BP	0.0401298171424475
	GO:0007377	germ-band extension	BP	0.0401298171424475
	GO:0070403	NAD+ binding	MF	0.0401298171424475
	GO:0035186	syncytial blastoderm mitotic cell cycle	BP	0.0401298171424475
	GO:0004972	N-methyl-D-aspartate selective glutamate receptor activity	MF	0.0401298171424475
	GO:0007059	chromosome segregation	BP	0.0401298171424475
	GO:0007370	ventral furrow formation	BP	0.0422451376177311
	GO:0000775	chromosome, centromeric region	CC	0.0422451376177311
	GO:0051233	spindle midzone	CC	0.0422451376177311
	GO:0000086	G2/M transition of mitotic cell cycle	BP	0.0422451376177311
	GO:0006412	translation	BP	0.0427362647342411
	GO:0019706	protein-cysteine S-palmitoyltransferase activity	MF	0.046899415605028
	GO:0031532	actin cytoskeleton reorganization	BP	0.046899415605028
	GO:0035025	positive regulation of Rho protein signal transduction	BP	0.046899415605028
	GO:0003735	structural constituent of ribosome	MF	0.046899415605028
	GO:0016226	iron-sulfur cluster assembly	BP	0.046899415605028
	GO:0050770	regulation of axonogenesis	BP	0.0484208269709028
	GO:0016328	lateral plasma membrane	CC	0.0488578254290042
	GO:0016476	regulation of embryonic cell shape	BP	0.0488578254290042

Supplementary Table S3. Preprocessing and mapping. Samples were prepared in biological triplicate. totalSequences, number of sequenced reads; tooShort, number of reads shorter than 14 base pairs; tooManyN, number of reads containing more than 2 N bases; totalPassed, tooShort and tooManyN subtracted from totalSequences; mapped, number of reads mapped to the *P. vanderplanki* genome; unmapped, number of reads not mapped to the same genome; MappingRate, proportion of mapped reads among all passed reads.

	Preprocess Result				Mapping Result		
	totalSequences	tooShort	tooManyN	totalPassed	mapped	unmapped	MappingRate
T0-Sample1	9329152	1089685	33	8239434	1682490	6556944	20.4
T0-Sample2	8618767	1642930	23	6975814	2463740	4512074	35.3
T0-Sample3	5486398	1002516	12	4483870	1517136	2966734	33.8
T48-Sample1	8249645	907419	27	7342199	1282918	6059281	17.5
T48-Sample2	4527055	923602	9	3603444	1340121	2263323	37.2
T48-Sample3	5862177	1172255	20	4689902	1747773	2942129	37.3
D8-Sample1	7162127	867901	23	6294203	1263235	5030968	20.1
D8-Sample2	5497776	914899	15	4582862	1384844	3198018	30.2
D8-Sample3	4710977	789877	19	3921081	1214370	2706711	31.0
D10d-Sample1	9786341	972550	49	8813742	1410369	7403373	16.0
D10d-Sample2	5046272	887863	13	4158396	1358339	2800057	32.7
D10d-Sample3	6176969	1146552	21	5030396	1716458	3313938	34.1
R3-Sample1	2269038	431391	3	1837644	687580	1150064	37.4
R3-Sample2	1966504	340563	6	1625935	533487	1092448	32.8
R3-Sample3	4409262	614660	6	3794596	1188580	2606016	31.3
R24-Sample1	3580658	819575	8	2761075	1228917	1532158	44.5
R24-Sample2	5913507	1330397	16	4583094	2078353	2504741	45.3
R24-Sample3	5071881	1122334	14	3949533	1752922	2196611	44.4